

INTERNATIONAL CENTRE FOR THEORETICAL PHYSICS

34100 TRIESTE (ITALY) - P.O.B. 586 - MIRAMARE - STRADA COSTIERA 11 - TELEPHONE: 7940-1
CABLE: CENTRATOM - TELELEX 440882 - I

SME/206-8

"SCHOOL ON POLYMER PHYSICS"27 April - 15 May 1987"HIGH-RESOLUTION ELECTRON MICROSCOPY OF VIRGIN
POLY(TETRAFLUOROETHYLENE)"Professor Henri D. ChanzyC.E.R.M.A.V.

Martin d'Heres, France

These are preliminary lecture notes, intended only for distribution to participants.
Missing or extra copies are available in Room 231.

High-Resolution Electron Microscopy of Virgin
Poly(tetrafluoroethylene)

HENRI D. CHANZY* and PAUL SMITH†, *E. I. du Pont de Nemours & Company, Inc., Central Research and Development Department, Experimental Station, Wilmington, Delaware, 19898 USA and*
JEAN-FRANCOIS REVOL, *Pulp & Paper Research Institute of Canada, Pulp & Paper Building, McGill University, 3420 University Street, Montreal, P.Q., H3A 2A7 Canada*

Virgin poly(tetrafluoroethylene) (PTFE) has some unusual physical properties (cf. ref. 1) such as a very high melting point, a high degree of crystallinity,² and remarkable flow properties.³ These properties indicate that the polymer as-polymerized contains very few topological defects.⁴ Indeed, it has been suggested that virgin PTFE is comprised of extended chain crystallites. This suggestion is corroborated by results obtained in various morphological and structural studies⁵⁻⁸ of PTFE dispersions. In these investigations it has been demonstrated that virgin PTFE dispersions consist of various kinds of particles; most of these particles are nonuniform spherical entities having dimensions in the range from 0.1 to 0.5 μm , whereas a minor fraction of the particles occurs as rods. The latter have previously been shown to be extended-chain crystals with the chain axis parallel to the long axis of the rods.⁷ The structure of the "spherical" particles has been suggested to be irregularly folded ribbons.⁷ With the advancement of electron microscopic techniques, such as lattice imaging, it has become possible to provide more conclusive evidence for these hypotheses. In this article we present the results of a low dose, high-resolution, electron microscopic study of the morphology of virgin poly(tetrafluoroethylene) dispersion particles.

Common PTFE dispersion was used throughout this study. No special specimen preparation techniques were employed. Droplets of diluted dispersion were placed onto carbon-coated 400 mesh grids and the dispersion medium (water) was allowed to evaporate at room temperature. These specimens were examined both in a Jeol 200CX and a Philips 400 T electron microscope.

The Jeol instrument was operated at 200 kV and was employed for conventional imaging and electron diffraction. In order to avoid damaging of the highly beam sensitive PTFE (see e.g. ref. 9) electron microscopy was carried out at low irradiation dose. The dose was monitored using a Gatan analytical sample holder fitted with a Faraday cup. In some experiments the irradiation dose was purposely increased in order to visualize and record beam damage.

Lattice imaging was performed at 120 kV with the Philips electron microscope that was equipped with a low dose attachment. This setup permitted maintaining high resolution even at low magnification. Photomicrographs were recorded with the low-dose unit of never-examined areas of the specimen. For each photograph a cumulative dose of 1 electron/ \AA^2 was selected. High-resolution images were recorded at a magnification of 46,000 and at a defocus setting of about 1000 \AA . The exposure time was 2 sec;

*Permanent address: C.E.R.M.A.V. (CNRS), B.P. 68, 38402 Saint Martin d'Heres Cedex, France.

†Present address: University of California, Department of Chemical and Nuclear Engineering, Materials Program, Santa Barbara, CA 93106.

an ILFOSET emulsion (ILFORD, France) was used, which was developed in concentrated D19 Kodak developer. The high-resolution micrographs were scanned on a laser bench in order to detect areas that contained periodic arrangements. Such areas were enlarged 15 times using a Wild-Leitz Photomicroscope. The enlargements were recorded on 35-mm Kodalith Ortho 6556 emulsion, which was developed in concentrated D19. These negatives were used as intermediates for the final enlargement.

Figure 1 shows electron micrographs of typical virgin PTFE dispersion particles. The micrograph of Figure 1A displays the rodlike structures described in the introduction. The insert in Figure 1A is a selected-area electron diffraction pattern of the framed single rod; it is properly oriented with respect to the image. The pattern can readily be indexed as an a^*c^* section of the reciprocal lattice of PTFE in its room temperature polymorph form. The rod axis is parallel with c^* and perpendicular to a^* . Four strong reflections are found along a^* at 0.49, 0.24, 0.16, and 0.12 nm, which index as (100), (200), (300), and (400), respectively.¹⁰ Along c^* , only one strong reflection is present at 0.13 nm, corresponding to (0013). Other features of the pattern are the sharp (1013) and streaked (101) and (107) reflections.

The electron micrograph in Figure 1B is of the "spherical" particles found in the same dispersion. Typical dimensions of these structures are of the order of 0.2 μm . Micrograph 1C is an enlarged view of one spherical particle. This particle exhibits two wedge-shaped dark regions arising from diffraction contrast. Figure 1D shows the selected-area diffraction pattern of the particle in Figure 1C, in proper orientation. The pattern consists of individual (100) diffraction spots in two small arcs corresponding to the two dark diffracting areas of the particle. Within these areas the PTFE chains are tangentially oriented with respect to the particle. The "spotty" nature of the diffraction pattern and the narrow line width are indicative of a very high degree of crystalline order in relatively large domains. The electron micrographs of Figure 1B reveals no consistent shape, size, or position of the dark Bragg extinction areas within the particles.

High-resolution electron micrographs of the rodlike PTFE particles are displayed in Figure 2. The micrograph of Figure 2A is a low magnification overview of a number of rods. A high-resolution image of a single rod (framed in 2A) is presented in Figure 2B. The figure displays well-resolved 0.49-nm lattice fringes (corresponding to the (100) spacings of PTFE¹⁰ throughout the entire width of the rod. These fringes appear to be continuous along the rod axis over a distance of approximately 0.1 μm , despite some slight bending. Figure 2C shows an enlarged section. It is illustrative of the perfection of the crystalline lattice within the rods, in complete agreement with the well-documented high crystallinity of virgin PTFE.² The lattice images were analyzed by optical diffraction (see insert in Fig. 2A). The optical diffractogram is similar to the electron diffraction pattern in Figure 1A, with the exception that the diffraction information in the former is limited to spacings exceeding about 0.2 nm due to the image resolution of the electron microscope used. Accordingly, the optical diffractogram of Figure 2A consists of only the (100) and (200) diffraction spots.

Plate 3 displays a set of micrographs of spherical PTFE particles. The high-resolution lattice image of Figure 3B is observed within the area of the particle that is in diffraction contrast. The lattice fringes, which appear less evident than in the rods, are curved along the boundary of the particle and are indicative of the tangential arrangement of the polymer chains. The corresponding optical diffractogram is presented in the insert in Figure 3B. Note its close resemblance with the electron diffraction pattern in Figure 1B.

Figure 4 displays an electron micrograph of spherical PTFE particles that were beam etched with a cumulative dose of 40 electrons/ \AA^2 . This picture reveals many different convoluted arrangements of rods, presumably within the spherical particles. PTFE, like many other organic polymers, is highly sensitive to electron beam damage.¹¹ This fluoropolymer rapidly degrades and simply evaporates under the vacuum in the

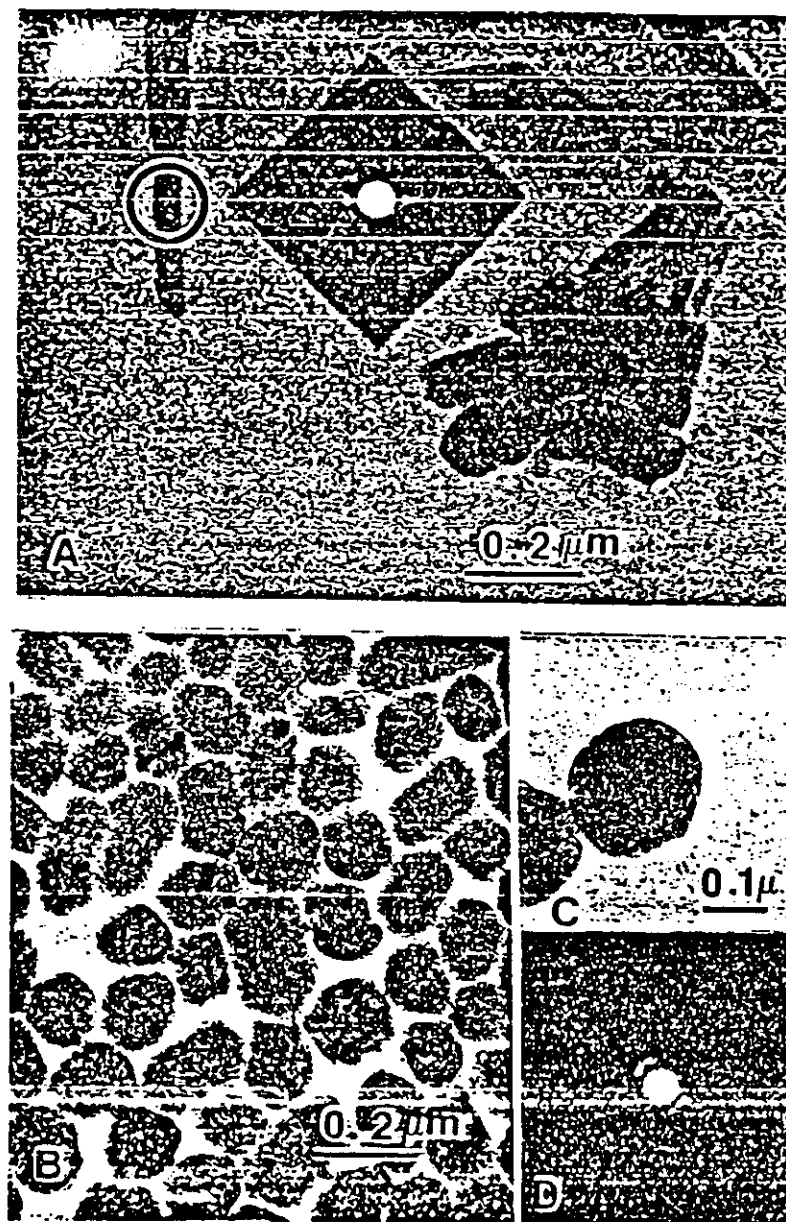


Fig. 1. A—Transmission electron micrograph of PTFE dispersion comprised of spherical and rodlike particles. Insert: electron diffraction pattern of a single rod (framed area). B—Electron micrograph of spherical PTFE dispersion particles. Dark wedge-shaped zones within particles arise from diffraction contrast. C—Enlarged micrograph of a single particle displaying two diffracting areas. D—Electron diffraction diagram of particle in 1C, properly oriented with respect to the image.

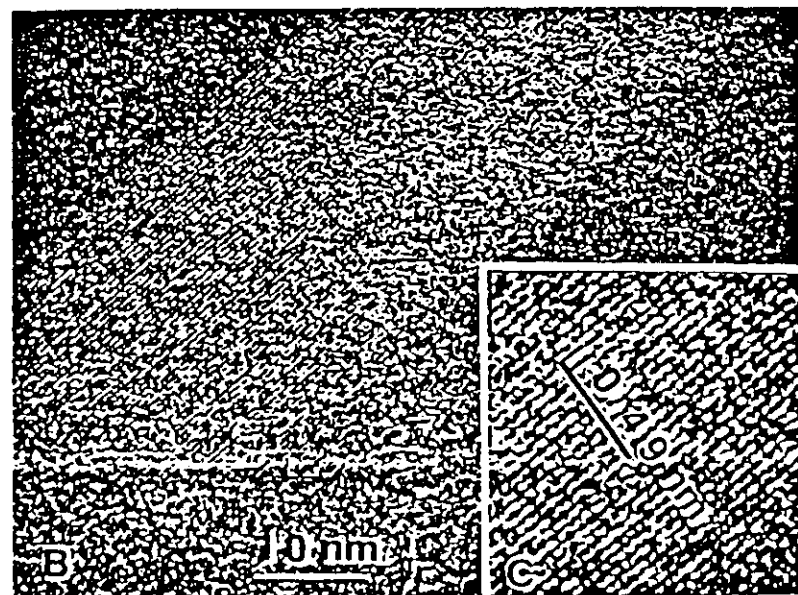
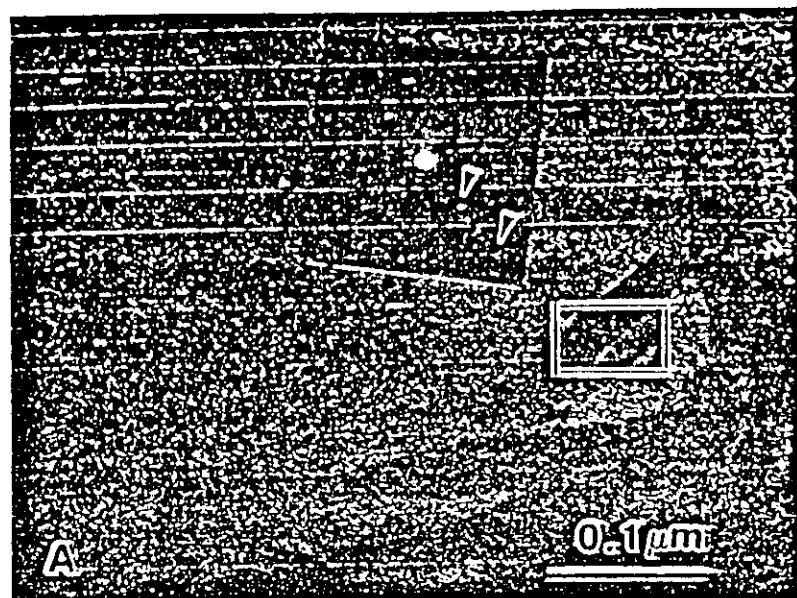


Fig. 2. A—Low-dose, high-resolution electron micrograph of real-like PTFE particles. Insert: laser beam diffractogram of the framed area of the original negative of photograph 2A. B—Enlargement of framed area in 2A, printed in negative contrast, resolving lattice fringes. C—Enlarged area of 2B.

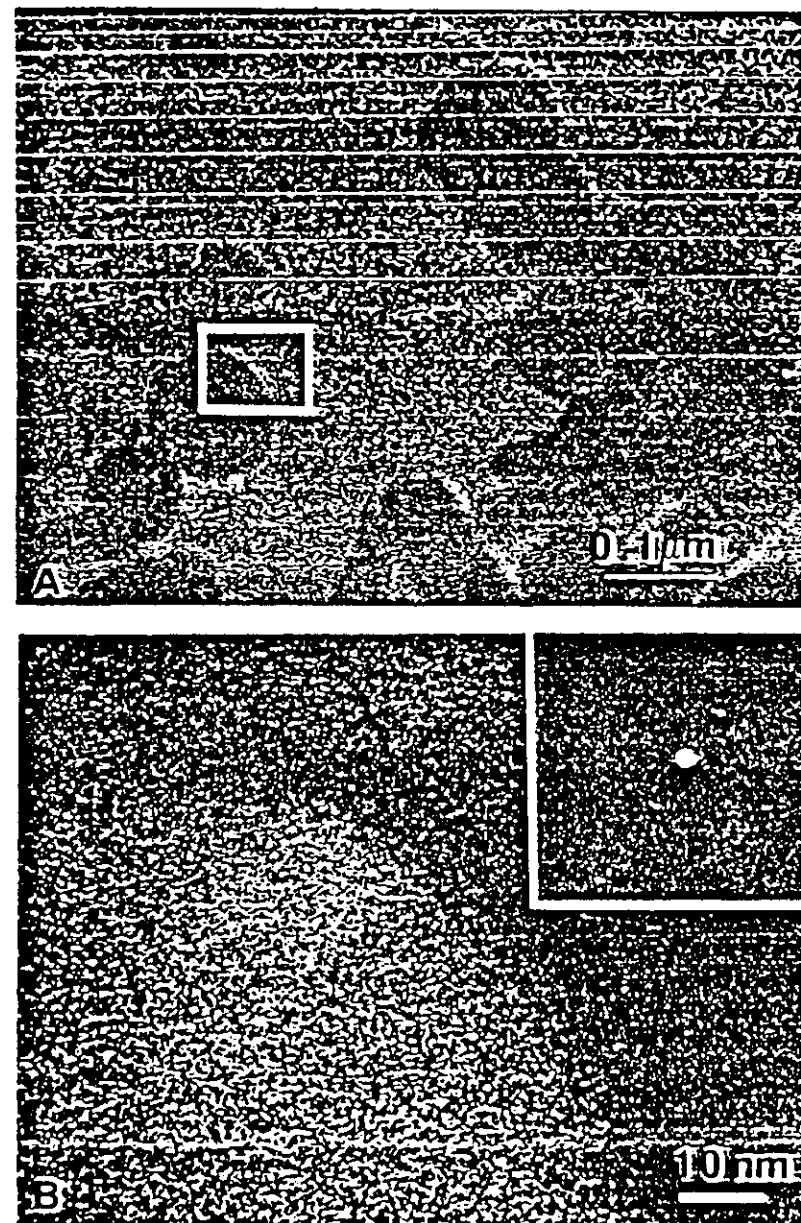


Fig. 3. A—Low-dose, high-resolution electron micrograph of PTFE dispersion displaying spherical particle. B—Enlargement of framed area, negative contrast. Insert: optical diffractogram of the bright zone in diffracting contrast in 3B.

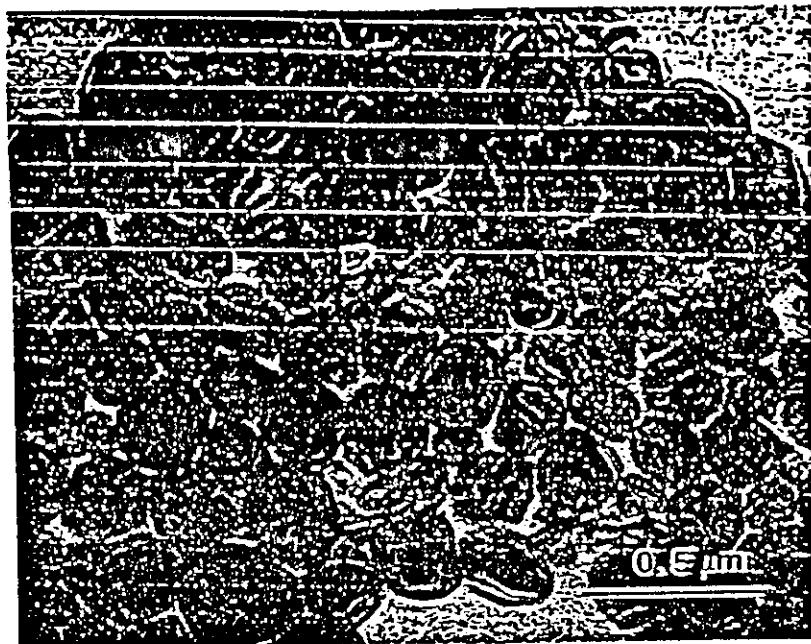


Fig. 4. Transmission electron micrograph of PTFE dispersion of particles that had been beam etched at 200 kV with a cumulative dose of 40 electrons/Å².

electron microscope, which, in principle, permits to "etch away" successive layers of the particles. The danger of introducing artifacts with this technique is significant, and the micrograph of Figure 4 cannot be interpreted without caution.

The electron micrographs and diffraction patterns presented above indicate that the rodlike particles present in virgin PTFE dispersion are fully extended chain crystals containing few defects. The spherical particles appear to be composed of similar rodlike entities which are wrapped around themselves in a more or less random fashion. These conclusions are in agreement with electron diffraction and morphological information obtained in earlier studies.⁷ The lattice images presented in this paper are, however, more conclusive. They directly reveal the local chain orientation, the size of crystalline domains, and the presence of defects.

The mechanism by which tetrafluoroethylene polymerizes into extended-chain crystals can readily be envisaged. PTFE is commercially produced by free-radical polymerization in the presence of water and a surfactant. The surfactant is present to increase the solubility of the monomer in the reaction medium and to stabilize the growing polymer particles. The polymerization is carried out at a temperature of about 80°C. This temperature is far below the dissolution temperature of PTFE in any solvent¹¹ and therefore the polymerization proceeds under conditions similar to a gas phase polymerization;^{12,13} at no instant during the polymerization is the growing polymer chain, or any significant portion, in the liquid state. Thus the macromolecules have no freedom to adopt a coiled conformation or to fold back onto themselves: under these conditions of near simultaneous polymerization and crystallization, extended-chain crystals are usually obtained (for an excellent review cf. ref. 14). The question remains as to why both rods and spherical particles are observed. This issue has been

previously discussed by Suwa et al.,¹⁵ who proposed a molecular weight dependent polymerization mechanism. Our view¹⁴ is that the final form of the PTFE dispersion particles is primarily dictated by the concentration of surfactant that is used in the polymerization. It is generally accepted that rodlike particles are generated in the initial stages of the polymerization⁷ and the spherical structures in a later stage. The initially formed rodlike particles are stabilized by the surfactant. As long as surfactant is available to encapsulate the growing rods, this mode of particle growth continues. Transformation into spherical entities occurs when the surfactant/polymer concentration ratio is no longer sufficient. At this point rodlike particles are unstable since they would experience the very high water/PTFE surface tension and collapse.

It is a pleasure to thank Dr. H. W. Starkweather, Jr., and Dr. A. D. English for many helpful discussions and critical reading of the manuscript. The authors also wish to express their gratitude to Dr. T. Folda for supplying PTFE samples.

References

1. C. A. Sperati and H. W. Starkweather, Jr., *Fortschr. Hochpolym.-Forsch.*, **Bd. 2**, 465 (1961).
2. H. W. Starkweather, Jr., P. Zoller, G. A. Jones, and A. J. Vega, *J. Polym. Sci. Polym. Phys. Ed.*, **20**, 751 (1982).
3. H. W. Starkweather, Jr., *J. Polym. Sci. Polym. Phys. Ed.*, **17**, 73 (1979).
4. A. J. Vega and A. D. English, *Macromolecules*, **13**, 1635 (1980).
5. C. W. Bunn, A. J. Cobbold, and R. P. Palmer, *J. Polym. Sci.*, **28**, 365 (1958).
6. P. H. Geil, *Polymer Single Crystals*, Wiley-Interscience, New York 1963, p. 481.
7. F. J. Fahl, M. A. Evanco, R. J. Fredericks, and A. C. Reimschuessel, *J. Polym. Sci., A-2*, **10**, 1337 (1972).
8. T. Seguchi, T. Suwa, N. Tamura, and M. Takahisha, *J. Polym. Sci. Polym. Phys. Ed.*, **12**, 2567 (1974).
9. E. Grimaud, J. Sanlaville, and M. Troussier, *J. Polym. Sci.*, **31**, 525 (1958).
10. C. W. Bunn and E. R. Howells, *Nature*, **18**, 549 (1954).
11. C. A. Sperati, in *Polymer Handbook*, 2nd ed., J. Brandrup and E. H. Immergut, Eds., Wiley, New York, 1975, p. V-29.
12. G. Butanuth, *Verhandl. Kolloid-Ges.*, **18**, 168 (1958).
13. L. Melillo and B. Wunderlich, *Kolloid Z. Z. Polym.*, **250**, 417 (1972).
14. B. Wunderlich, *Adv. Polym. Sci.*, **5**, 568 (1968).
15. T. Suwa, T. Seguchi, M. Takahisha, and S. Machi, *J. Polym. Sci. Polym. Phys. Ed.*, **13**, 2183 (1975).
16. T. Folda, H. Hoffmann, H. D. Chanzy, and P. Smith, *Nature*, to be submitted.

Received January 28, 1986

Accepted March 20, 1986

Journal of Materials Science Letters

Journal of Materials Science Letters is an international publication reporting recent advances in all the major fields of investigation into the properties of materials. Short communications on metallurgy, ceramics, polymers, electrical materials, biomaterials, composites and fibres appear regularly.

Letters for submission to the *Journal of Materials Science Letters* should be sent to Professor W. Bonfield, Dept. of Materials, Queen Mary College, Mile End Road, London E1 4NS.

Journal of Materials Science Letters is published monthly by Chapman and Hall Ltd., 11 New Fetter Lane, London EC4P 4EE, as a combined subscription with *Journal of Materials Science*. Subscription details are available from: Subscriptions Department, Associated Book Publishers Ltd., North Way, Andover, Hampshire SP10 5BE. Telephone: Andover (0264) 62141.



CHAPMAN AND HALL

H. CHANZY*, T. FOLDA†, P. SMITH, K. GARDNER

E.I. du Pont de Nemours and Company, Inc., Central Research and Development Department, Experimental Station, Wilmington, Delaware 19898, USA

J.-F. REVOL

Pulp and Paper Institute of Canada, 570 St-John's Boulevard Pointe Claire, Québec, Canada H9R 3J9

Electron microscopy and, in particular, diffraction-contrast electron microscopy has been an important tool in the study of the supra-molecular structure of crystalline polymers [1, 2]. In the last few years the resolution of electron microscopes has been improved to the point that it has become possible to analyse crystals at a molecular level, provided that the material is sufficiently resistant to the electron beam [3–5]. This technique, commonly referred to as lattice imaging, has not been applied to polymers until recently; it is expected to yield a wealth of structural information such as direct views on the shape of projected macromolecules, local orientation of crystalline blocks and even molecular defects within crystals.

Lattice images have been presented in the literature of several polymers that are relatively resistant to the electron beam [3–12] and, very recently, of polymeric materials that are more sensitive to beam damage, such as cellulose [12, 14] and polyethylene [15].

The present work deals with lattice imaging of poly(tetrafluoroethylene) (PTFE) single crystals. This study was prompted by the observation that in several conventional tetrafluoroethylene polymerizations a substantial amount of single crystals was produced, especially in the early stages of the reactions.

An aqueous dispersion of "as-polymerized" PTFE, sampled at the very early stage (conversion (1%) of a conventional tetrafluoroethylene emulsion polymerization [16] was used in this study. The dried material was found to exhibit a very sharp melting point of 270°C (differential scanning calorimetry at a scan speed of 10°C min⁻¹). This temperature is well below the melting point of about 345°C that is commonly observed for the as-polymerized high polymer; it is estimated to correspond to the melting temperature of extended chain crystals of PTFE having a chain length of about 60 C-atoms (MW = 3000) [17, 18].

Drops of the PTFE dispersion were deposited on 400-mesh electron microscope grids covered with a 10-nm-thick carbon film. The specimens were allowed to dry and were subsequently examined in a Philips EM 400T electron microscope. This instrument was operated at an accelerating voltage of 120 kV and was equipped with a low-dose unit. Electron micrographs were recorded of never-examined areas of the specimen at a plate magnification of 46000 and using under-focusing conditions of around 100 nm. An

exposure time of 2 sec was selected; the illumination conditions were controlled to deliver an accumulated dose of only 200 electrons nm⁻² to the specimen. The images were recorded on ilfovet emulsion (Ilford, France) and developed in 5 min with Kodak D19 full-strength developer. The electron micrographs were recorded with an optical density between 0.4 and 0.6.

Optical diffraction patterns of the micrographs were obtained using a Polaron electronmicrograph optical diffractometer. Regions of the micrographs that displayed optical diffraction of the highest resolution and symmetry were selected for further photographic enlargement. These intermediate negatives were scanned on a Photomat PI700 microdensitometer (Optronics, Inc., Chelmsford, Mass.) using a 50-µm raster, resulting in an effective sampling of the material of ~0.04 µm. Regions of 480 × 480 pixels, corresponding to 19.2 × 19.2 nm² were digitized, fast-Fourier transformed, filtered and back transformed, to produce a filtered image. For the computer processing of the images, the micrograph processing software package (MDPP) [19], running on a DEC VAX 11/750 (under VMS 4.1), was used.

A general view of the as-polymerized PTFE oligomer crystals is presented in Fig. 1. The crystals appeared as platelets having a lateral dimension of about 100 nm. They had geometrical shapes, such as hexagons and truncated lozenges with obtuse angles of 120°. Electron diffraction revealed that the chain axis was perpendicular to the crystal surface. The thickness of the crystals ranged from about 50 nm, where they were transparent, to higher values as was inferred from their opacity to the electron beam. This range of the crystal thickness corresponds to extended chain lengths of perfluoroalkanes having 40 C-atoms or more, which agrees reasonably well with the number of CF₂-units that was deduced from the melting point.

A typical high-resolution/low-dose electron micrograph of an individual crystal is shown in Fig. 2a. Examination of the micrograph by optical diffraction yielded a diffractogram (insert) comprising six sharp spots organized in hexagonal symmetry. The spots were found at a *d* spacing of 0.49 nm, which corresponds to the (100) spacing of PTFE in its room temperature crystalline polymorph [20].

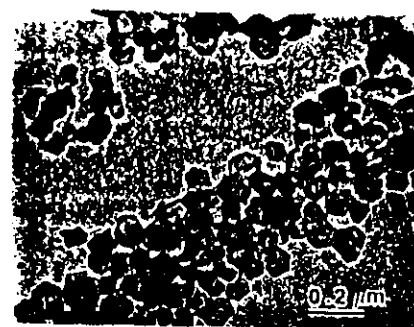


Figure 1 Typical electron micrograph of a dispersion of "as-polymerized" oligomeric poly(tetrafluoroethylene) (PTFE) single crystals.

An enlargement of the crystal in Fig. 2a is shown, in reverse contrast, in Fig. 2b. At this magnification, a fine and rather regular honeycomb structure was observed throughout the crystal. A further enlargement, in direct contrast, is presented in Fig. 3. Three sets of lattice fringes crossing at an angle of 120° can be detected in these figures, despite a significant noise level due to grain in the photographic film and to the structure of the carbon support film. Reduction of this noise was achieved by the image-enhancement method described above. Upon Fourier-transforming the digitized image, a pattern in all respects similar to the optical transform was obtained. A filter of 5 × 5 pixels was constructed around each reflection and the back transform was produced. This filtered image is shown in the insert of Fig. 3. This figure shows a well-resolved lattice consisting of rows of hexagonally packed white circular dots. The row of dots are 0.49 nm apart and correspond to the projection of individual PTFE chain molecules. Remarkably, no defect or dislocation appeared to be present in the original micrograph and in the computer-processed image.

The results presented in this letter demonstrate that (oligomeric) PTFE can be successfully analysed by high-resolution electron microscopy, in spite of the

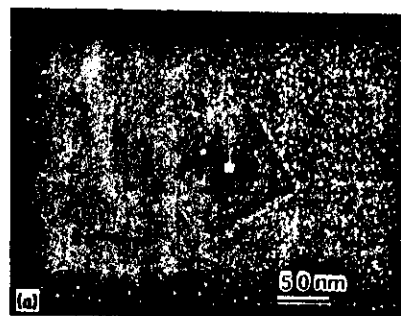


Figure 2 (a) Low-dose electron micrograph of one PTFE single crystal and its optical diffractogram (insert). (b) Enlargement of (a) in reverse contrast.

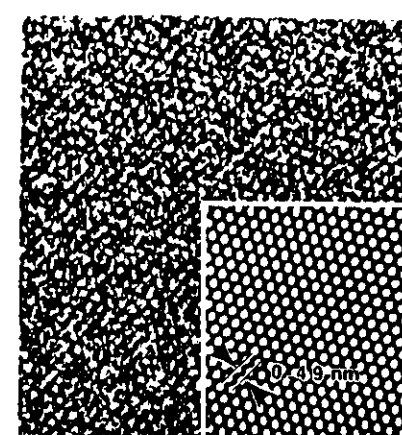


Figure 3 Further enlargement (same contrast as in Fig. 2a) of computer-filtered image (insert).

known electron beam sensitivity of this material [2]. More specifically, lattice imaging, revealing 1.049 nm spacing, seems to be possible. The chain molecules, viewed in projection, had the expected [2] circular shape. More details at higher resolution could not be obtained, however, because images such as Fig. 3 were produced with interferences having a spacing of 0.49 nm, which naturally limits the resolution to this value. The next equatorial *d* spacing of the PTFE crystal lattice occurs at 0.28 nm [2]. Presently, this spacing and its corresponding lattice image cannot be resolved.

Acknowledgement

The authors thank Dr H. W. Starkweather Jr for helpful comments.

References

1. D. T. GRUBB, in "Development in Crystalline Polymers" edited by D. C. Bassett (Applied Science, London, 1982).
2. E. L. THOMAS, in "The Structure of Crystalline Polymers", edited by I. A. Hall (Elsevier, New York, 1964) p. 1.
3. A. KELLER, *Kolloid Z., U.Z. Polymere* 231 (1969) 389.

* Permanent address: CERMAV (CNRS), BP 68, 38402 Saint Martin d'Hères Cedex, France.

† Present address: Norcon Materials, 1440 N. Kraemer Blvd., Anaheim, California 92806, USA.

12. T. READ and R. J. YOUNG, *J. Mater. Sci.* 16 (1981) 22.
13. J. YOUNG and P. N. J. YEUNG, *J. Mater. Sci.* 16 (1981) 1327.
14. K. KATAYAMA, *Polymer* 22 (1981) 1568.
15. ISODA, M. TSUJI, M. OHARA, A. KAWAKUCHI and K. KATAYAMA, *ibid.* 24 (1983) 1155.
16. G. DOBB, D. J. JOHNSON and B. P. SAVILLE, *J. Appl. Polym. Sci., Polym. Symp.* 36 (1977) 237.
17. KATAYAMA, S. ISODA, J. TSUJI, M. OHARA and A. KAWAGUCHI, *Bull. Inst. Chem. Res., Kyoto Univ.* (1984) 198.
18. ISODA, M. TSUJI, M. OHARA, A. KAWAGUCHI and K. KATAYAMA, *Makromol. Chem., Rapid Commun.* (1983) 141.
19. KAWAGUCHI, S. ISODA, J. PETERMANN and KATAYAMA, *Colloid Polym. Sci.* 262 (1984) 429.
20. N. UYEDA, *Makromol. Chem.* 30 (1964) 98.
21. J. F. REVOL, *J. Mater. Sci. Lett.* 4 (1985) 1347.
22. J. F. REVOL and R. ST-JOHN MANLEY, *ibid.* 5 (1986) 249.
23. C. A. SPERATI and H. W. STARKWEATHER Jr., *Adv. Polym. Sci.* 2 (1961) 465.
24. P. SMITH and K. H. GARDNER, *Macromolecules* 10 (1965) 1222.
25. H. W. STARKWEATHER Jr., *ibid.* in press.
26. P. R. SMITH, *Ultramicroscopy* 3 (1978) 153.
27. C. W. BUNN and E. R. HOWELLS, *Nature* 173 (1954) 549.
28. F. GRIMAUD, J. SANLAVILLE and M. TROUSSIER, *J. Polym. Sci.* 31 (1958) 525.

Received 21 March
and accepted 21 April 1986

J.-F. REVOL AND H. CHANZY, *Pulp and Paper Research Institute of Canada, 3420 University Street, Montreal, Quebec H3A 2A7, Canada, and Centre de Recherches sur les Macromolécules Végétales, B.P. 68, 38402, St. Martin d'Hères Cedex, France*

Lattice imaging is rapidly becoming an important tool for the investigation of the morphology of crystalline synthetic and natural polymers. Recently, it has been shown that the technique is not limited only to polymers that are resistant to electron beams such as Kelvar,¹ polyparaxylylene,² and polymeric sulfur nitride [(SN)_x]_n,³ but that it also can be applied to substances of intermediate resistance such as the isotactic polystyrene,⁴ and those of very low resistance such as polyethylene⁵ or teflon (H. Chanzy, J.-F. Revol, and P. Smith, in preparation). It has also been found that native polymer microfibrils such as those of *Valonia* cellulose, can yield high-resolution lattice images.^{6,7} In this case, the photomicrographs gave evidence for a highly perfect lattice ordering within the cellulose microfibrils. In particular, no substructure, either parallel or perpendicular to the microfibril direction, could be detected and it was concluded that each *Valonia* microfibril is in fact a crystalline cellulose whisker of high perfection.

The present study deals with the high-resolution electron microscopy of β -chitin microfibrils, which bear a close resemblance to cellulose microfibrils. Samples from the spines of *Thalassiosira fluxuatis* were selected for study since these display a high crystallinity together with the absence of contaminating proteins.

A dried preparation of the spines from the diatom *Thalassiosira fluxuatis* was kindly provided by Dr. R. Colvin.⁸ The specimen was immersed overnight in a 50/50 (v/v) solution of concentrated HCl in methanol. After thorough washing in methanol, the sample was dispersed by sonication. Drops of the resulting suspension were allowed to dry on 400 mesh electron microscope grids covered with a carbon film 10 nm in thickness. The electron microscope used was a Philips EM400T instrument operated at the accelerating voltage of 120 kV and equipped with a low-dose unit.⁹ The photomicrographs were recorded at a magnification of 60,000 \times on Ilfoset film (ILFORD, France). An exposure time of 2 s was chosen and the corresponding accumulated electron dose necessary to record one picture was 2.5 C/ μm^2 (1.56 e⁻/ \AA^2). The photomicrographs, which were developed for 5 min in full-strength D-19 Kodak developer, were subsequently analyzed with a Polaron electron micrograph optical diffractometer.

A representative electron micrograph of β -chitin preparation is shown in Fig. 1. Long microfibrils are seen with widths ranging from 10 to 30 nm. Very often several microfibrils associated laterally to form larger ribbons. The optical diffraction pattern shown as an inset in Fig. 1 comes from the framed area. It exhibits reflections corresponding to a portion of the a^*c^* projection of the reciprocal lattice of β -chitin as defined by Gardner and Blackwell.¹⁰ The two reflections 002 and 004 along the c^* axis and the 100 reflection along the a^* axis are clearly visible. An enlargement of the framed area of Fig. 1 is shown in Fig. 2. Lattice lines are clearly seen in the two directions parallel and perpendicular to the microfibril axis, with corresponding spacings of 0.48 nm and 0.52 nm. This set of crossed lattice lines can be followed along the

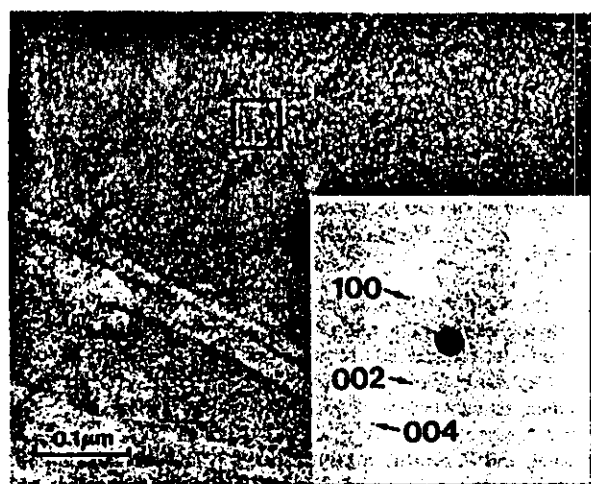


Fig. 1. Electron micrograph of a dispersion of β -chitin microfibrils from the spines of *Thalassiosira fluviatilis*. Inset: Optical diffraction pattern of the framed area.

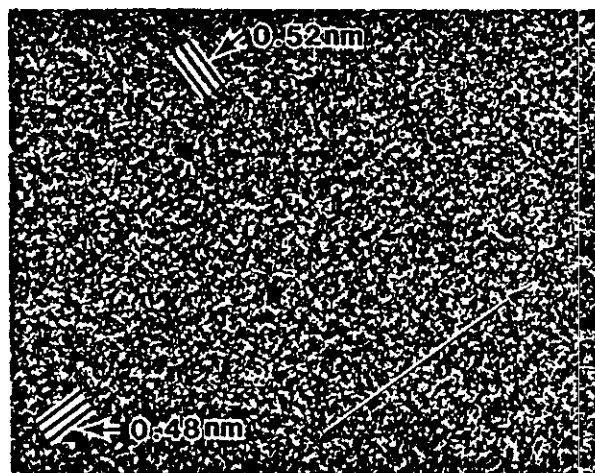


Fig. 2. Enlargement of the framed area of Fig. 1. The arrow points toward the axis of the microfibril.

microfibril over distances exceeding 100 nm. Although the lattice lines corresponding to the (004) planes, with spacing of 0.26 nm, cannot be seen on the picture, they are clearly detected in the optical diffraction of Fig. 1. This is due to the low signal-to-noise ratio resulting from the limited dose of electrons used to record the image, together with the granularity of the photographic emulsion. An improvement of the signal-to-noise ratio by spatial filtering of the image transform, either optically or by computer, would probably allow these lattice lines to be clearly revealed.

The results presented here show that there is a similarity between cellulose microfibrils, as in the *Valonia* cell wall, and β -chitin microfibrils from the diatom spines of *Thalassiosira fluviatilis*. In both cases, the microfibrils are true polymeric crystalline whiskers with the chains aligned, and probably fully extended, along the microfibril axis over large domains. As found for *Valonia* cellulose,^{6,7} the chitin microfibrils do not display any lateral substructure such as elementary fibrils or subelements. This implies that the observation of such subelements after mechanical shearing¹¹ is the result of a longitudinal disruption of the original extended chain crystals.

The β -chitin lattice images such as those shown in Fig. 2 exhibit better resolution than those published so far for cellulose. This is due to the higher resistance of chitin to electron-beam irradiation. With the use of 120-keV electron beams, it thus appears feasible to resolve all the chitin lattice lines within 0.3–0.25 nm resolution. In particular, with the a^*c^* projection of β -chitin, at least five different lattice lines giving reflections of strong and medium intensities should be detected. Work is presently in progress to obtain such lattice images, the goal being to achieve the molecular resolution by using image processing (J.-F. Revol, K. H. Gardner, H. Chanzy, in preparation).

References

1. Dobb, M. G., Hindeleh, A. M., Johnson, D. J. & Saville, B. P. (1975) *Nature* **253**, 189–190.
2. Tsuru, M., Isoda, S., Ohara, M., Kawaguchi, A. & Katayama, K. (1982) *Polymer* **23**, 1568–1574.
3. Karaguchi, A., Isoda, S., J. Petermann, J. & Katayama, K. (1984) *Polym. Sci.* **262**, 429–434.
4. Tsui, M., Roy, S. K. & Manley, R. St. J. (1984) *Polymer* **25**, 1573–1576.
5. Revol, J.-F. & Manley, (1986) *R. St. J. J. Materials Sci. Lett.* **5**, 249–251.
6. Sugiyama, J., Harada, H., Fujiyoshi, Y. & Uyeda, N. (1984) *Mokuzai Gakkaishi* **30**, 98–99.
7. Revol, J.-F. (1985) *J. Materials Sci. Lett.*, **4**, 1347–1349.
8. Dwellitz, N. E., Colvin, M. R. & McInnes, A. G. (1968) *Can. J. Chem.* **46**, 1513–1521.
9. *Low-Dose Unit for EM400*. (1979). Handbook. Philips. Eindhoven-The Netherlands.
10. Gardner, K. H. & Blackwell, J. (1975) *Biopolymers* **14**, 1581–1595.
11. Gardner, K. H. & Blackwell, J. (1971) *J. Polym. Sci. C* **36**, 327–340.

Received November 15, 1985

Accepted March 4, 1986

HIGH-RESOLUTION ELECTRON MICROSCOPY OF ULTRADRAWN
GELS OF HIGH MOLECULAR WEIGHT POLYETHYLENE

H.D. Chanzy

C.E.R.M.A.V. (CNRS), B.P. 68, 38402 Saint Martin d'Heres Cedex, France

Paul Smith

University of California, Department of Chemical and Nuclear Engineering,
Materials Program, Santa Barbara, CA 93106, U.S.A.

J.-F. Revol and R. St. John Manley

Pulp & Paper Research Institute of Canada, 570 St. John's Boulevard, Poincaré
Claire, PQ, Canada H9R 3J9 and McGill University, Department of Chemistry,
Montreal, PQ, Canada H3A 2A7

ABSTRACT

High-resolution electron microscopy was performed on ultradrawn gel-films of high molecular weight polyethylene. Micrographs featuring lattice line information were produced under selected microscope conditions. These lattice images were found to be substantially more informative than conventional bright- and dark-field images. Structural information was obtained from these images such as the position of the crystalline blocks within the ultrathin films, their identification i.e. orthorhombic or triclinic crystal form, and their exact orientation with respect to the drawing direction.

KEYWORDS

HIGH-RESOLUTION ELECTRON MICROSCOPY, HIGH-MODULUS POLYETHYLENE, STRUCTURE

1

INTRODUCTION

Recently, substantial progress has been made in high-resolution electron microscopy of crystalline polymers (1). This advanced imaging is particularly spectacular for electron-beam sensitive polymers (2-6). These developments prompted us to reinvestigate the structure of ultra-high modulus polyethylene, with the objective of imaging these unusual materials (7-10) at the molecular level. Indeed, it is at this resolution that insight is required to develop an understanding of the factors that determine their mechanical properties. In this report we present some preliminary results showing lattice images of high-modulus films produced by drawing polyethylene gels (e.g. ref. 10, 11). The films were specially prepared for direct examination by transmission electron microscopy. As expected, the high-resolution images reveal new features that are not observed by standard diffraction-contrast electron microscopy (12-16).

EXPERIMENTAL

Ultra-high molecular weight polyethylene (UHMWPE) (Hercules Hifax 1900, $\bar{M}_w \sim 5 \times 10^6$) was used throughout this study. Solutions of 1% w/w of UHMWPE were prepared at 160°C in decalin. In order to reduce degradation of the polymer 0.1% w/w of the antioxidant Irganox 1010 was added. The solutions were cast at room temperature to form gel films. These gel films were allowed to dry at ambient temperature. Rectangular strips of 50 mm x 5 mm were cut from the dried films. These specimens were mounted in an Instron tensile tester that was equipped with a temperature regulated oven. The

films were drawn at a crosshead speed of 10 mm/min. The final draw ratio was measured from the displacement of ink marks printed onto the samples prior to deformation. A first series of samples was drawn to a draw ratio of 60x at 128°C; a second series 25x at 70°C. The drawn films, which had an average thickness of around 0.1 μ m, were floated on water. Small sections were cut from the films with a dissecting knife and mounted on carbon-coated 400 mesh electron microscope grids. A layer of carbon having a thickness of about 5 nm was evaporated onto the specimens in order to improve their stability and prevent charging under electron irradiation.

Electron microscopy was performed with a Philips EM 400T instrument that was equipped with a low-dose unit. The instrumental conditions used were identical to those described elsewhere (4). Photomicrographs were recorded at a magnification of 36,000x on Ilfoset (Ilford, France) films. These micrographs, which had an optical density of around 0.5, were scanned with a Polaron optical diffractometer. Regions of the micrographs that displayed optical diffraction patterns were enlarged 15 times on Kodak electron microscope film (4489). These enlargements were scanned with the optical diffractometer and each crystalline block that corresponded to a diffraction spot was identified and its contours marked. The optical diffractograms were calibrated using images, also recorded at 36,000x, of graphitized carbon black as a standard.

RESULTS AND DISCUSSION

The micrograph in Figure 1A, taken in the bright-field mode, illustrates the corrugated appearance of the 60 times drawn polyethylene films.

This corrugation is inferred from the succession of white and dark filaments that are encountered upon scanning the films perpendicular to the draw direction which is indicated by the arrow. These thread-like domains, which have a width of about 50 nm and a length of several microns, are almost perfectly aligned along the draw direction. The difference in contrast from one domain to the next is due to differences in thickness. The thickness is estimated to be a few tenths of a nm for the clearer areas and at least 100 nm in the darker regions. When a square micron of the film shown in Figure 1A is probed by electron diffraction, the pattern in Figure 1B is obtained. This pattern corresponds to a fiber diffraction diagram of polyethylene, with near perfect chain orientation along the draw axis. Analysis of the diagram in Figure 1B reveals information related mostly to the orthorhombic polyethylene phase. A small amount of triclinic phase (17) is also present, as is evidenced by the faint pair of 010 spots diffracting at a d-spacing of 0.45 nm. Figure 1C is a typical dark-field image produced with the 110 and 200 diffracting beams from orthorhombic polyethylene together with the 010 from the triclinic phase. This dark-field micrograph indicates that within each of the elongated domains seen in Figure 1A, there is a succession of irregularly shaped bright areas (polyethylene crystalline blocks which produce the diffracted beams previously mentioned) with dimensions of the order of 40 to 60 nm. These observations, obtained here on extremely thin films, are in full agreement with our previous work dealing with thicker ultradrawn polyethylene films, examined by high-voltage electron microscopy (16).

Lattice images of the same specimen were obtained at magnifications as low as 36,000x. This was achieved by combining low-dose imaging techniques with instrumental conditions where a resolution of at least 0.3 nm is main-

tained, even at such low magnification. Examples of lattice images are presented in Figures 2-4. Figure 2A displays a region of the 60 times drawn polyethylene film. When this micrograph is analyzed by optical diffraction, spots are detected that correspond to the (110) planes of polyethylene at a spacing of 0.31 nm. This is illustrated in the optical diffractogram from the framed area in Figure 2A (inset). This diagram exhibits one pair of sharp spots aligned perpendicular to the drawing direction. An enlargement of the framed area in Figure 2A is presented in Figure 2B. At this magnification, the lattice lines are visible almost throughout the entire photograph, i.e. over distances of at least 40 nm along the drawing direction and 20 to 30 nm across. The lattice lines which run diagonally are aligned parallel to the drawing direction without apparent dislocation, which reveals the high perfection of the polyethylene crystals contained in such ultradrawn films.

In Figure 3A, the optical diffraction diagram (inset) corresponds to the entire area of the image which was obtained from the 60 times drawn film. Two pairs of sharp reflection spots aligned perpendicular to the stretching direction are present with spacings of 0.41 nm and 0.45 nm, corresponding to the orthorhombic and triclinic crystal structures respectively. This shows that the chain axis of the two polymorphs contained in Figure 1A is parallel to the drawing direction. Figure 3B, obtained as described in the experimental part, is a schematic illustration of the triclinic and orthorhombic domains localized in two elongated regions in close contact. The triclinic domain is over 50 nm in length and 15 nm in width. The orthorhombic area is of comparable length but has a width of 10 nm. The very low signal-to-noise ratio does not allow us to determine the exact

nature of the transition zone between the two phases. However the crystalline domains are in very close contact since the gap between the two defined regions is less than 1 nm.

The image of Figure 4A was obtained on the polyethylene film that was stretched 25 times, at 70°C. In this image adjacent crystalline blocks, featuring lattice lines at 0.41 nm spacing and misoriented with respect to one another by approximately 2 degrees, are clearly revealed by the splitting of the reflection spots in the corresponding optical diffractogram (inset). By laser-beam scanning the image of Figure 4A, we were able to outline the contours of two crystalline blocks (Figure 4B). In this figure there is a small block on the left, with dimensions of 40 nm along the drawing direction and 25 nm perpendicular to it. The block on the right is larger; it extends over 70 nm along the drawing direction and 40 nm across. As was deduced from the optical diffractogram in Figure 4A, the two blocks are misaligned by about 2 degrees. Unlike the domains in Figure 3, these two blocks appear not to be in close contact, except perhaps at a very localized spot where lattice information is essentially unexisting.

By conventional diffraction contrast in the dark-field mode several diffracted beams are frequently selected simultaneously with the objective aperture. As a result, and in particular for structures having a fibre symmetry, the imaged crystalline domains cannot be identified. When lattice imaging is performed the interference between the central beam and the diffracted beams produces lattice lines from each corresponding crystal. Accordingly, a subsequent optical analysis of the resulting images will identify these individual crystalline blocks, showing the full potential of this technique. For example, in Figure 3, it is possible to localize

exactly the triclinic phase and to differentiate it from the orthorhombic, while in Figure 4, a slight misorientation of two crystalline blocks is clearly seen.

Finally, it is interesting to note that within all the (irregularly shaped) crystalline blocks observed, the lattice lines are perfectly straight. Particularly illustrative in this respect are the micrographs taken from the 25 times drawn specimen. Misalignment between two adjacent crystalline blocks is clearly observed by optical diffraction and lattice imaging (see Figure 4A and 4B). Within each crystalline block, the polyethylene macromolecules are perfectly aligned, however, and the misorientation is confined between the crystalline blocks rather than within them. This observation is in contrast with related studies on poly(tetrafluoroethylene) (5), where curved lattice lines were frequently encountered. This finding seems to indicate that polyethylene crystals have a higher "flexural modulus" than poly(tetrafluoroethylene) crystals.

ACKNOWLEDGEMENTS

Part of the experimental work was carried out by two of us (H.D.C. and P.S.) during their stay at the Central Research & Development Department of E. I. du Pont de Nemours & Company, Inc. The help of Sylvie Peyre Smith in the preparation of the manuscript is greatly appreciated.

*that it explains an well understood that these of P.E.E.
without disruption of their
which can bend easily without any
alignment.*

REFERENCES

1. Katayama, K., Isoda, S., Tsuji, H., Ohara, M. and Kawaguchi, A. Bulletin Institute for Chemical Research, Kyoto University 1984, 62, 198.
2. Sugiyama, J., Harada, H., Fujiyoshi, Y. and Uyeda, N. Mokuzai Gakkaishi 1984, 30, 98.
3. Revol, J.-F. J. Mater. Sci. Lett. 1985, 4, 1347.
4. Revol, J.-F. and St. John Manley, R. J. Mater. Sci. Lett. 1986, 5, 249.
5. Chanzy, H.D., Smith, P. and Revol, J.-F. J. Polym. Sci. Polym. Lett. 1985, 24, 557.
6. Revol, J.-F. and Chanzy, H.D. Biopolymers 1986, 25, 1599.
7. Southern, J.H. and Porter, R.S. J. Appl. Polym. Sci. 1970, 14, 2305.
8. Capaccio, G. and Ward, I.M. Polymer 1974, 15, 233.
9. Zwiijnenburg, A. and Pennings, A.J. J. Polym. Sci. Polym. Lett. 1976, 14, 339.
10. Smith, P. and Lemstra, P.J. J. Mater. Sci. 1980, 15, 505.
11. Smith, P., Lemstra, P.J., Pijpers, J.P.L. and Kiel, A.M. Colloid & Polymer Sci. 1981, 259, 1070.
12. Zwiijnenburg, A., Van Hutten, P.F., Pennings, A.J. and Chanzy, H.D. Colloid & Polymer Sci. 1978, 256, 729.
13. Capaccio, G. and Ward, I.M. J. Polym. Sci. Polym. Phys. 1981, 19, 667.
14. Grubb, D.T. and Hill, M.J. J. Cryst. Growth 1980, 48, 321.
15. Sherman, E.S., Porter, R.S. and Thomas, E.L. Polymer 1982, 23, 1069.

16. Smith, P., Boudet, A. and Chanzy, H.D. J. Mater. Sci. Lett. 1985, 4, 13.
17. Turner-Jones, A. J. Polym. Sci. 1962, 62, S 53.

FIGURE CAPTIONS

Figure 1A - A Polyethylene Transmission electron micrograph of a 160x drawn film prepared at 120°C. The arrow indicates the drawing direction.

B - Electron diffraction diagram of an area of one square micron. The arrow points toward a diffraction spot corresponding to a spacing of 0.45 nm, which is indicative of the presence of a small amount of the triclinic polyethylene crystal modification.

C - Dark-field electron micrograph obtained with the equatorial diffraction spots 110 and 200 of the orthorhombic phase and the 010 spot of the triclinic crystal phase.

Figure 2A - Low-dose electron micrograph of the stretched film of Figure 1A. Inset: optical diffractogram of the framed area. This diffractogram displays one pair of strong spots that correspond to the (110) planes of polyethylene in its orthorhombic form.

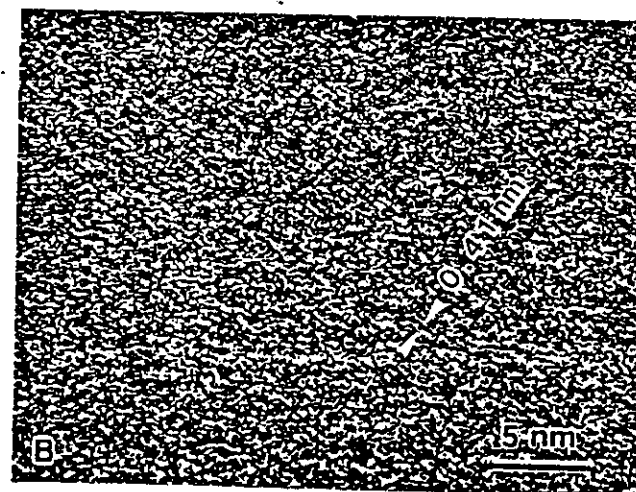
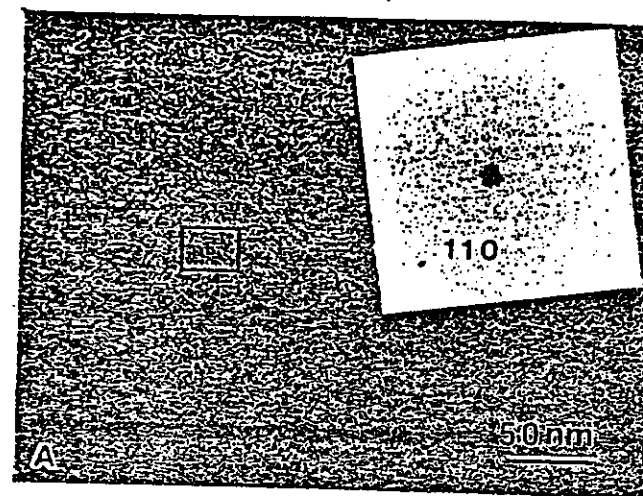
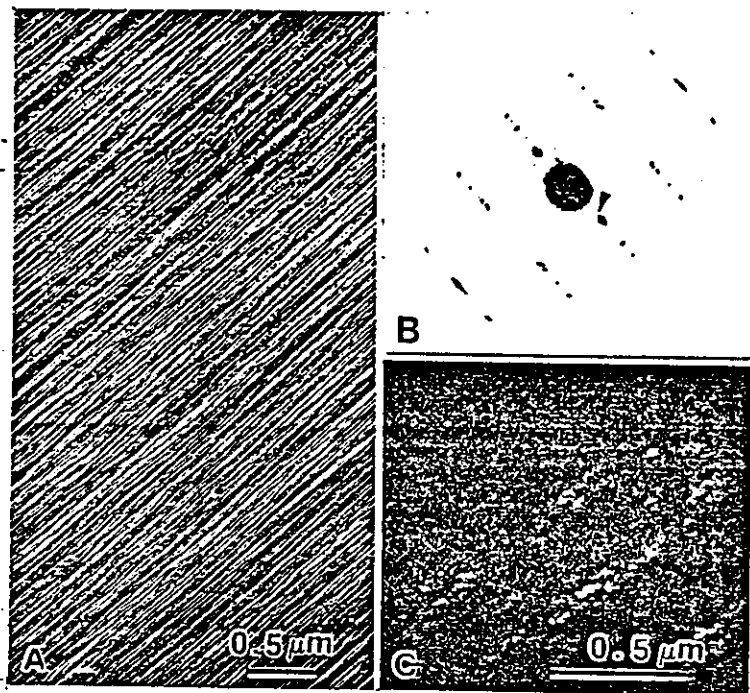
B - Enlargement of the framed area of Figure 2A. Lattice lines separated by 0.41 nm [(110) planes of the orthorhombic phase of polyethylene] are seen throughout the micrograph.

Figure 3A - Low-dose electron micrograph of the 60x drawn film. This micrograph contains lattice lines corresponding to 0.41 nm spacing [(110) planes of orthorhombic polyethylene], and lattice lines at 0.45 nm spacing [(010) planes of the triclinic phase], as shown by the optical diffractogram (inset).

B - Schematic diagram of Figure 3A, in which the contours of the orthorhombic and triclinic phases are outlined.

Figure 4A - Polyethylene low-dose electron micrographs of a 25x drawn film prepared at 70°C. Inset: corresponding optical diffractogram revealing a splitting of the 110 diffraction spot (0.41 nm spacing) of the orthorhombic crystal phase of polyethylene.

B - Schematic diagram of Figure 4A, in which the contours of the two crystalline blocks are outlined.



BoHan

CHANGYI et al.

BoHan

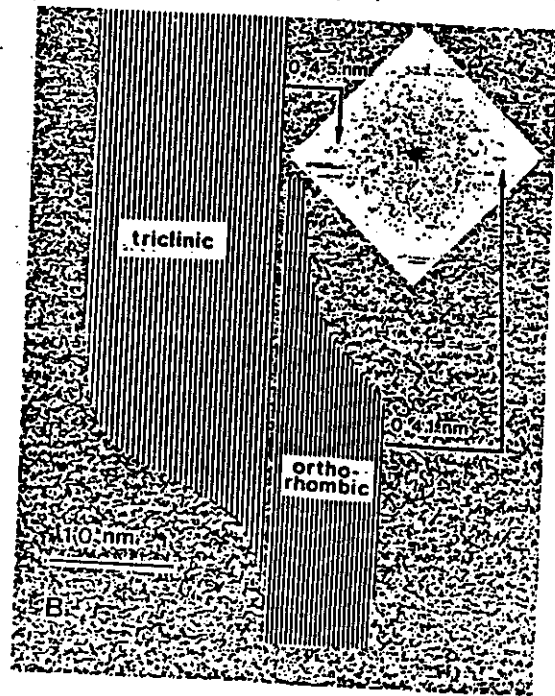
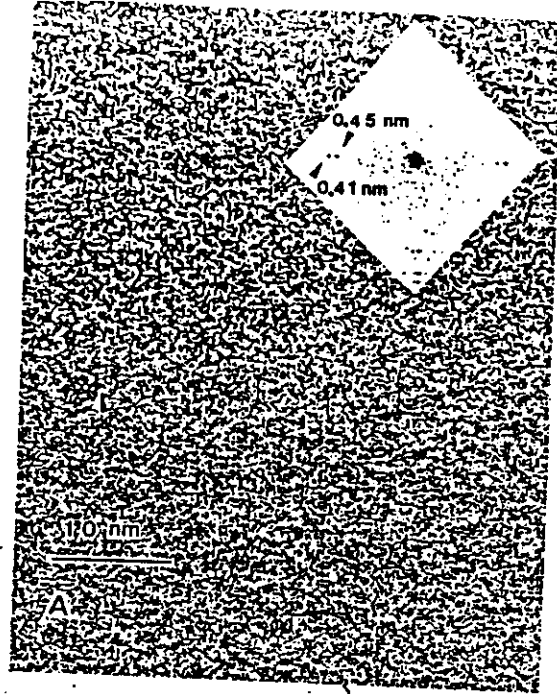
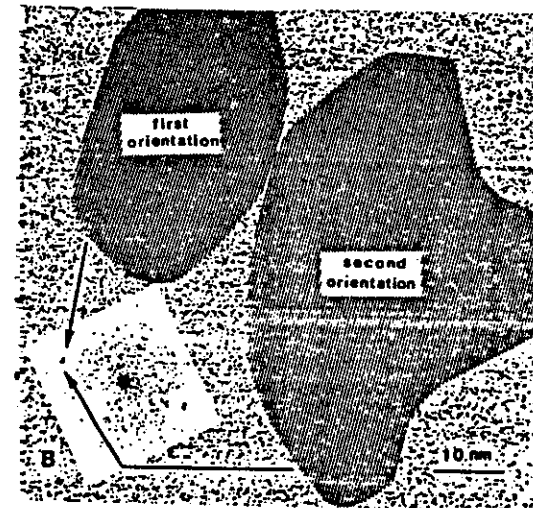
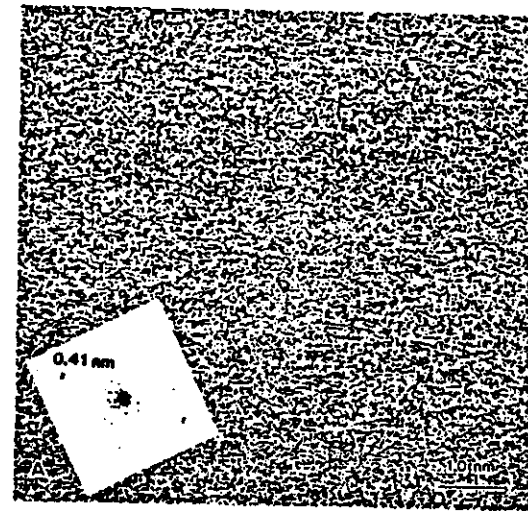


Figure 4



Han

CHAIZY et al.

R-A

β -CHITIN : MOLECULAR IMAGING AT 0.35 NM RESOLUTION BY
CONVENTIONAL ELECTRON MICROSCOPY

J.P. REVOL, K.H. GARDNER* and H. CHANZY**

Pulp and Paper Research Institute of Canada, and Department of Chemistry,
McGill University, 3420 University Street, Montreal, Quebec, Canada H3A2R7.

* Central Research and Development, Experimental Station, E.I. du Pont de
Nemours Inc., Wilmington, Delaware 19898, U.S.A.

** Centre de Recherches sur les Macromolécules Végétales (C.N.R.S.),
B.P. 68, 38402 Saint Martin d'Hères Cédex (France), affiliated with the
Scientific and Medical University of Grenoble (France).

Polymers are very sensitive to damage by electron beam radiation and as a consequence, high resolution electron microscopy of such materials has always been a tour de force. However, with recent developments in electron microscope, it is now possible to maintain high resolution at very low magnifications, where lower radiation dose can be used to record the images. This has led to several recent reports where lattice images were presented for synthetic and naturally occurring beam sensitive polymers 1-4. In particular, with β -chitin from the diatom Thalassiosira fluviatilis 5-6, electron micrographs showing lattice features having a resolution of 0.26 nm were recorded 7. More recently, with such specimen, we have obtained improved lattice images giving symmetric optical diffractograms of high quality. The present paper describes how these new images can be computer processed to yield an a*c* projection of the chitin chains in their crystalline environment, at 0.35 nm resolution. The reconstituted images are in good agreement with the known crystal structure of this polysaccharide 8-9 and in particular salient molecular details are clearly visualized.

A dried mat of pure chitin microfibrils from Thalassiosira-fluviatilis, originally prepared by J. McLachlan 5 was kindly forwarded to us by R. Colvin. The specimen was treated overnight in a 50/50 (v/v) solution of concentrated HCl in methanol. After washing in fresh methanol, the sample was dispersed by sonication. Drops of the resulting suspension were allowed to dry on 400 mesh electron microscope grids previously covered with 10 nm thick carbon films. The specimens were observed at 120 kV with a Philips 400T electron microscope equipped with a standard low dose unit which makes it possible to record pictures from un-irradiated areas, the focussing being carried out on an adjacent area. Ilfoset films from Ilford (France) were selected and the electron micrographs recorded on a never irradiated area of the specimen, at a magnification of 46,000X and with a 2 seconds exposure time, corresponding to a total accumulated electron dose of 1.5 elec./Å². Under such conditions, the films which were developed in Kodak D19 (full strength) for 5 minutes at 20°C had an optical density close to 0.5. They were then analyzed with a Polaron electron micrograph optical diffractometer. The regions of the films where β -chitin microfibrils produced diffraction patterns with good symmetry and high resolution were selected and enlarged 12 to 15 times on Kodak 4489 electron microscope films developed in Kodak D19 (diluted 1:2) for four minutes at 20°C.

These second negatives were then digitized with a Photomation P1700 microdensitometer (Optronics International, Inc., Chelmsford, MA) using a 25 micron raster resulting in an effective 0.04 nm sampling of the material. Typically regions of 800 x 800 pixels were digitized. Subarrays of 200 x 200 pixels were Fourier transformed to determine the regions of the original array that had the highest symmetry. Two adjacent subarrays which had shown the most highly symmetric diffraction patterns were combined for further analysis. Translational averaging of the 400 x 200 array was then performed to obtain an average unit cell. This unit cell showed an asymmetry between the contributions interpreted as the sugar residues. The unit cell was symmetrized with a glide parallel to the c axis (2-D equivalent to the 2_1 screw axis that is known to exist along the chain axis) and was used as a reference structure for cross-correlation. The result of the cross-correlation was a symmetrized unit cell that has been replicated to form the unit cell array shown in Figure 3. The digitized images were processed using the Micrograph Processing Software Package (MDPP)¹⁰.

A typical preparation of β -chitin microfibrils is shown in Figure 1a. The image, obtained by diffraction contrast, shows clearly individual microfibrils. These microfibrils have a width of up to 30 nm and show a strong tendency to associate and form wider ribbons as can be seen in the framed area in Figure 1a. Selected-area-electron diffraction on individual microfibrils gives rise to diffraction patterns such as the one presented in Figure 1b. This electron diffractogram exhibits sharp reflection spots which represent the a^*c^* projection of the reciprocal lattice. This pattern indicates that the individual microfibrils are single crystals of high perfection and that the fiber c axis is aligned with the microfibrils axis.

A careful optical diffraction analysis of this and similar micrographs reveals domains, such as in the framed area in Figure 1a, which produce a highly symmetric diffraction pattern. One such pattern is presented in Figure 1c. It is essentially the same diffractogram as that obtained with electrons but with a resolution limited to 0.35 nm instead of 0.1 nm that was observed on the original negative of Figure 1b. We previously reported lattice imaging of β -chitin with a resolution of 0.26 nm⁷, but in that case the optical diffractogram was not symmetric and therefore unsuitable for molecular imaging of the desired a^*c^* projection. The microfibril

corresponding to the non-symmetric diffraction pattern was not exactly oriented with the b axis perpendicular to the plane of observation. Rather, images of microfibrils producing optical diffraction patterns as shown in Figure 1c were preferred and digitized for further image processing.

Such an image is shown in Figure 2 along with the calculated Fourier transform of the image (inset in Figure 2). As expected, this transform is identical to the one recorded by optical diffraction. This indicates the presence of lattice lines corresponding to the (h0l) planes up to a resolution of 0.35 nm. However, it is difficult to observe these lines on the micrograph due to the very low signal-to-noise ratio. Indeed, the image was recorded at a very low dose of exposure resulting necessarily in a lack of electrons for the signal. In addition, the low magnification used (46,000X) introduces significant noise due to the granular nature of the photographic emulsion. For these reasons the molecular imaging can be extracted from the image only by noise filtering and by averaging of the resulting signal. A reconstructed image of the a^*c^* projection of β -chitin obtained by cross-correlation is presented in Figure 3, together with the a^*c^* projection of a β -chitin crystal calculated from the atomic coordinates given by Gardner and Blackwell⁹. The processed image and the molecular model are in good agreement. At this level of resolution (0.35 nm), features such as the conformation of the chitin macromolecule, its packing within the unit cell and even molecular details such as the C=O protuberance from the N-Acetyl moiety can be directly visualized.

The success of the present technique requires that the specimen is thin enough to be considered as a perfect phase object. The above β -chitin microfibrils meet this requirement since their thicknesses are of about 20 to 30 nm. Such crystals are not unique in the world of polysaccharides¹¹. The present work, which to our knowledge is the first attempt to obtain molecular imaging of a crystalline polysaccharide material, opens the way for further investigations with several other polysaccharides of biological or industrial importance.

REFERENCES

1. J. Sugiyama, H. Harada, Y. Fujiyoshi and M. Uyeda, *Mokuzai Gakkaishi*, **30**, 98 (1984).
- 2 J.F. Revol, *J. Materials Sci. Letters*, **4**, 1347 (1985).
3. J.F. Revol and R. St John Manley, *J. Materials Sci., Letters*, **5**, 249 (1986).
4. H. Chanzy, T. Folda, P. Smith, K. Gardner and J.F. Revol, *J. Materials Sci., Letters*, in press.
5. J. McLachlan, A.G. McInnes and M. Falk, *Canadian J. of Botany*, **43**, 707 (1965).
6. W. Herth and E. Schnepf in "Cellulose and other Natural Polymer Systems. Biogenesis, Structure and Degradation". R. Malcom Brown Jr. Edit., Plenum Press, New-York, 1982, p. 185.
7. J.F. Revol and H. Chanzy, *Biopolymers*, **25**, 1599 (1986).
8. J. Blackwell, *Biopolymers*, **7**, 281 (1969).
9. K.N. Gardner and J. Blackwell, *Biopolymers*, **14**, 1581 (1975).
10. P.R. Smith, *Ultramicroscopy*, **3**, 153 (1978).
11. H. Chanzy and R. Vuong in "Polysaccharides, Topics in Structure and Morphology", E.D.T. Atkins, Edit., Macmillan, London, 1985.

CAPTION FOR THE FIGURES

Figure 1

1a) Diffraction contrast electron micrograph of a dispersion of β -chitin microfibrils from the diatom *Thalassiosira-fluviatilis*. The contrast has been reversed during printing.

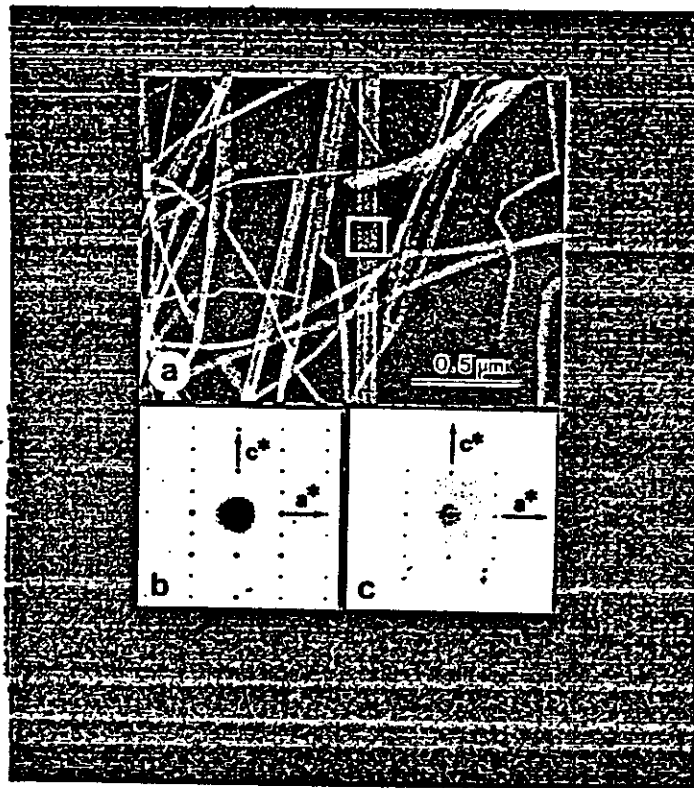
1b) Electron diffraction diagram representing the a^*c^* reciprocal lattice of one isolated β -chitin microfibril. Diffraction spots corresponding to spacings as low as 0.1 nm are visible on the original negative.

1c) Optical diffractogram from the framed area in Figure 1a. Diffraction spots corresponding to the 100 (0.48 nm), 101 (0.44 nm) 102 (0.35 nm) and 002 (0.52 nm) are clearly visible.

Figure 2 : Enlargement of the framed area in Figure 1a.

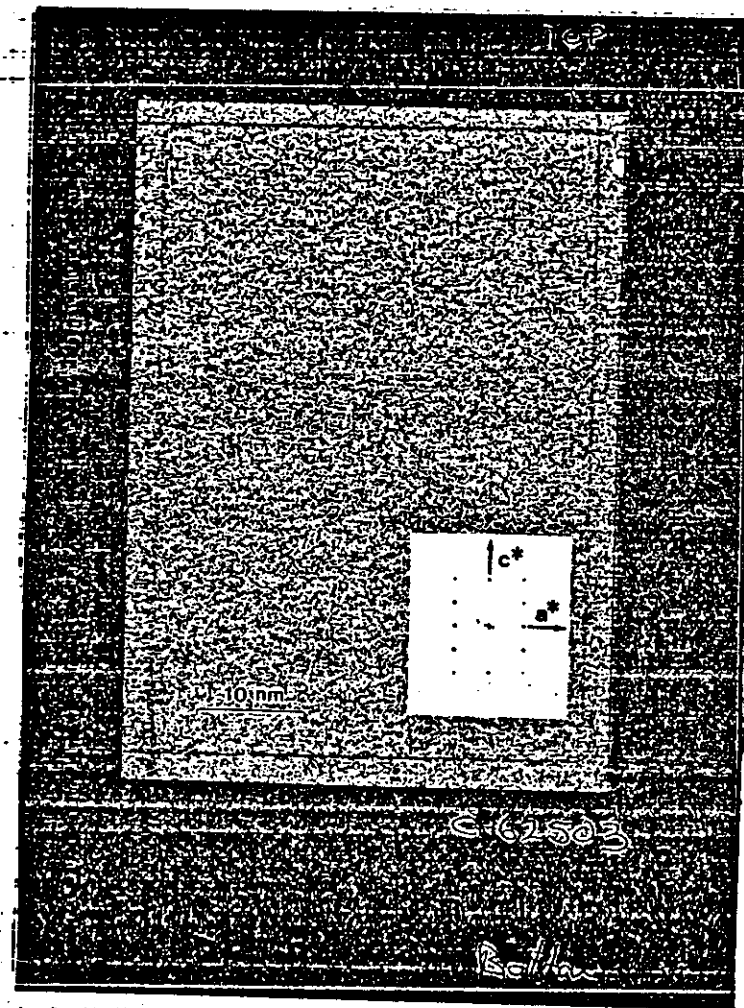
Inset : Corresponding computer calculated Fourier transform. This pattern is similar to the one obtained by optical diffraction in Figure 1c.

Figure 3 : Computer-reconstructed image of Figure 2 showing the projection of the β -chitin crystal along the b axis. Inset shows, at the same magnification, such a projection from the known crystallographic data⁸⁻⁹. In this model, the hydrogen atoms have been omitted for clarity, the carbon atoms are in black, the oxygen atoms in dark gray and the nitrogen atoms in light gray. There is a good agreement between the processed image and the projection derived from the crystallography.



C-62501

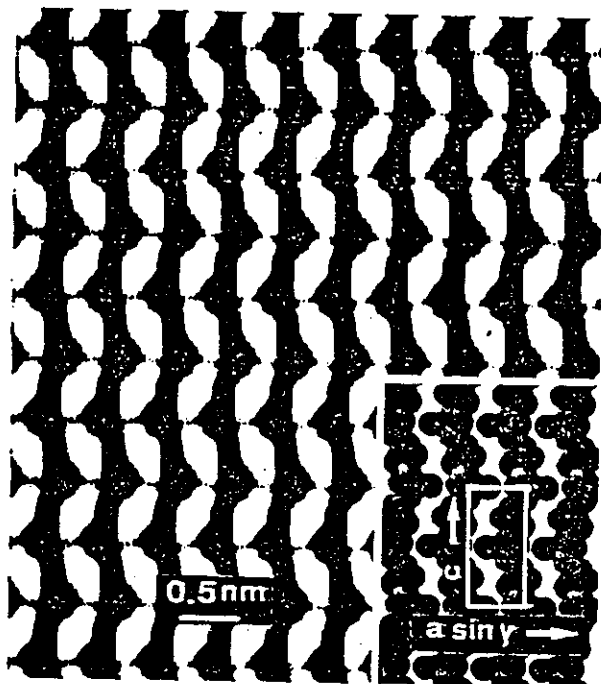
Rord et al. Figure 1 -



C-62503

Rord et al.

Rord et al, Figure 2



of al., Figure 3

Be 71a.

